

4. MULTI-SEGMENT NANORODS

4.1. Introduction

In the previous chapter, the conditions producing optimum control over the dimensions under which nanorods may be synthesized and efficiently collected were determined. These techniques will now be extended to the synthesis of nanorods with multiple metal segments (with a particular focus on bi-segmented nickel-gold nanorods) in order to acquire segmented nanorods that may be subsequently used in cross-phase alignment experiments with microphase separated diblock copolymer templates. Initial experiments will involve synthesis following “standard” literature conditions, which will serve as a control set of results for comparison with those nanorods produced in subsequent experiments that involve the application (and if necessary modification) of the optimised synthesis techniques developed in chapter 3. This will then be followed by experiments to determine the exact charge to segment length ratio for formation of the desired segmented nanorods, with a final experiment then to confirm that segmented nanorods suitable for use with block copolymer templates may be synthesised (desired dimensions / sufficiently small variation in dimensions as well as purity).

4.2. Experimental Methods and Materials

4.2.1. Membrane Preparation

Membrane template preparation is performed in the same manner as described in chapter 3 (section 3.2.1).

4.2.2. Nanorod Synthesis

Standard Conditions

Initial nanorod synthesis is performed using the same plating solutions and general literature procedure as outlined in chapter 3 (section 3.2.2), except that no nitric acid is used (brief sonication of the membrane template containing the deposited nanorods in methanol is used to remove the silver backing layer only) and metal is deposited in the order silver – nickel – gold – etc (the first nickel segment acting as a barrier layer between the sacrificial silver and gold nanorod segments). This is done so that the nanorods may be examined by TEM and EDAX to see how well the sequential deposition has proceeded (no loss or etching of segments).

Optimised Conditions

Experiments concerning the synthesis of nanorods using the optimized procedure developed in chapter 3 involve the following variations to the standard literature procedure:

- Specific order of metal deposition; silver – nickel – gold.
- Sonication during rinsing steps between metal depositions.

- Sonication during metal deposition.
- Metal deposition rate controlled by imposing an external current limit. In the case of gold, this limit is 1mA. No current limit is applied in the case of nickel deposition, as limiting the current in this case will result in an undesirable decrease in current density.
- Removal of the outer edge of the deposition area to account for variations in electric field strength over the cathode.

Note that, apart from the final experiment, all of these experiments have the majority of the membrane removed using a single centrifugation cycle as described in the standard literature procedure, as the nanorods synthesised in these experiments do not need to be free of polymer residue and this allows for faster analysis of the nanorods.

4.2.3. Nanorod Characterisation

Nanorod characterisation is performed in the same manner as described in chapter 3 (section 3.2.3).

4.3. Results and Discussion

4.3.1. Synthesis: Literature Conditions

TEM images of the segmented nanorods (0.05C Ni – 0.1C Au – 0.4C Ni – 0.1C Au), synthesised using the “standard” conditions described in section 4.2.2, are shown in fig 4.1. The vast majority of the resulting nanorods remain intact after collection by centrifugation, and appear to consist of well defined metal segments with diameters of < 80nm (larger diameter than previously observed due to the wider pores in the depth of the membrane template) and a similar range of segment lengths compared to individual nanorods that are synthesised under the same conditions. EDAX analysis of these metal segments (performed by focussing the electron beam of the TEM on each segment in turn and examining the resulting x-ray energy spectrum) confirms the composition and high purity of the individual segments (fig 4.2).

Importantly, these results indicate that no co-deposition of residual gold (remaining within the pores after rinsing) occurs during subsequent nickel deposition; a similar result to that noted during the deposition of gold following nickel in chapter 3. In this case, this appears to be due to the acidic nickel plating solution causing the residual gold cyanide species to be stripped of cyanide ligands (through the formation of HCN), leading to insoluble gold species that are then not electroplated. Taken together, these results show that judicious selection of the order of metal deposition is sufficient to obtain nanorods with compositionally pure metal segments for use in this work.



Fig 4.1: TEM image of a Ni-Au-Ni-Au segmented nanorod.

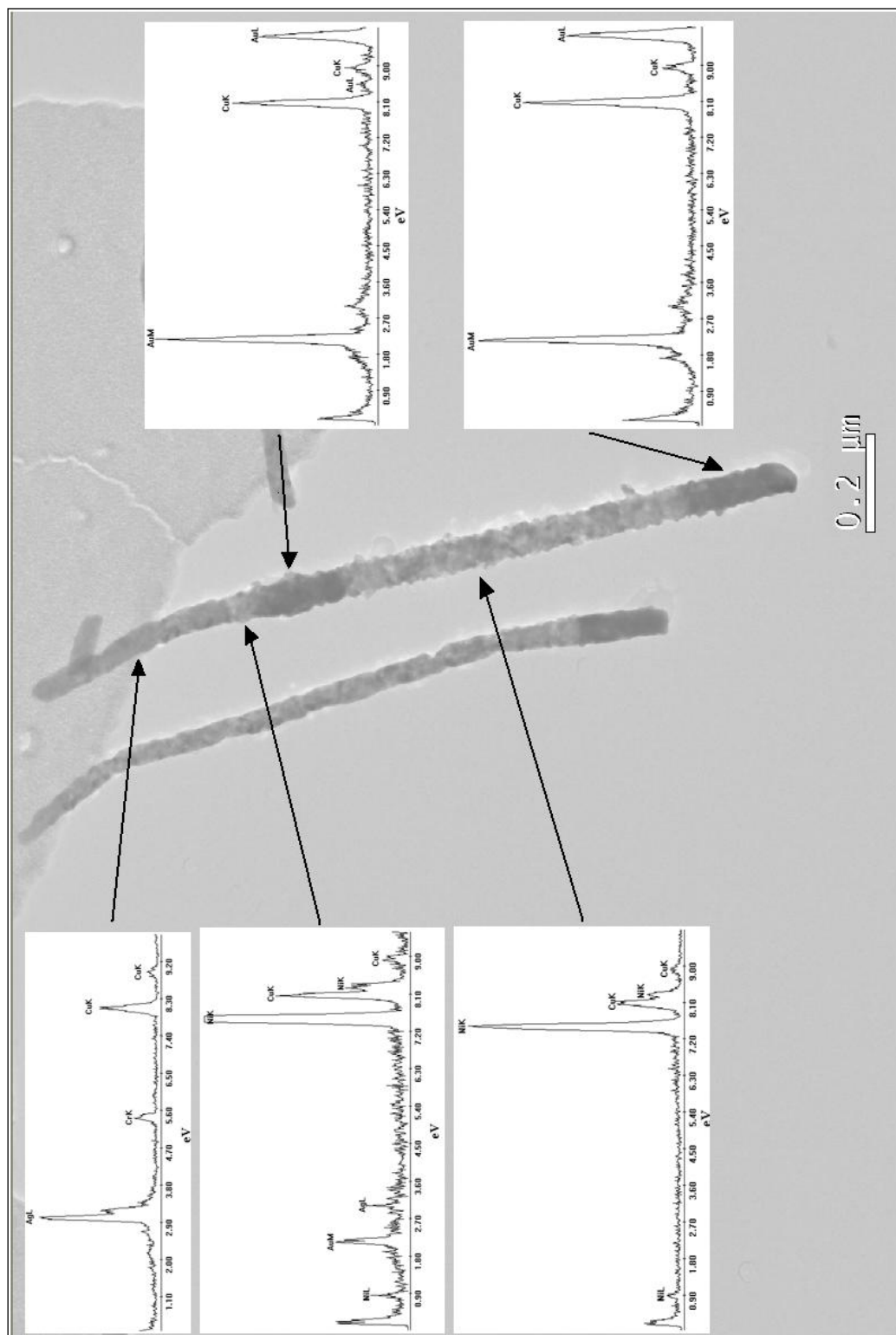


Fig 4.2: EDAX analysis of Ni-Au-Ni-Au segmented nanorods.

4.3.2. Synthesis: Optimised Conditions

TEM images of Ni-Au-Ni-Au segmented nanorods formed under optimised synthesis conditions are shown in fig 4.3. As can be observed, well defined nanorod segments have been formed under these conditions, with a range of segment lengths similar to that observed for single segment nanorods synthesised under the same conditions. However, the majority of the nanorods appear to have been broken into individual segments, most likely at the structurally weak segment interfaces.

Given that the segmented nanorods formed under standard conditions remain intact after collection, and knowing the differences in the synthesis procedures, the likely causes of the breakage of the nanorods are either related to the sonication and/or to the nitric acid treatment. Sonication during the synthesis could cause such breakage by applying sufficient stresses to the nanorods within the synthesis template to break the nanorods at the mechanically weak segment interfaces. [1-2] Nitric acid treatment could also lead to such breakage, by chemically attacking the nickel segments. The oxidation of the nickel that also occurs with treatment by concentrated nitric acid would limit such attack, but the small extent of dissolution may still be sufficient to weaken the adhesion between these segments at the nickel interfaces, such that applied forces (due to centrifugation) are now sufficient to break the nanorods (compounded by the relatively small diameter of these nanorods). This could even occur for nickel segments located between gold segments (which would be expected to protect the nickel from contact with nitric acid), as the thin PVP layer on the surface of the template pores is degraded by strong oxidisers (such as concentrated nitric acid), thereby allowing access to these nickel segments by the nitric acid (fig 4.4).

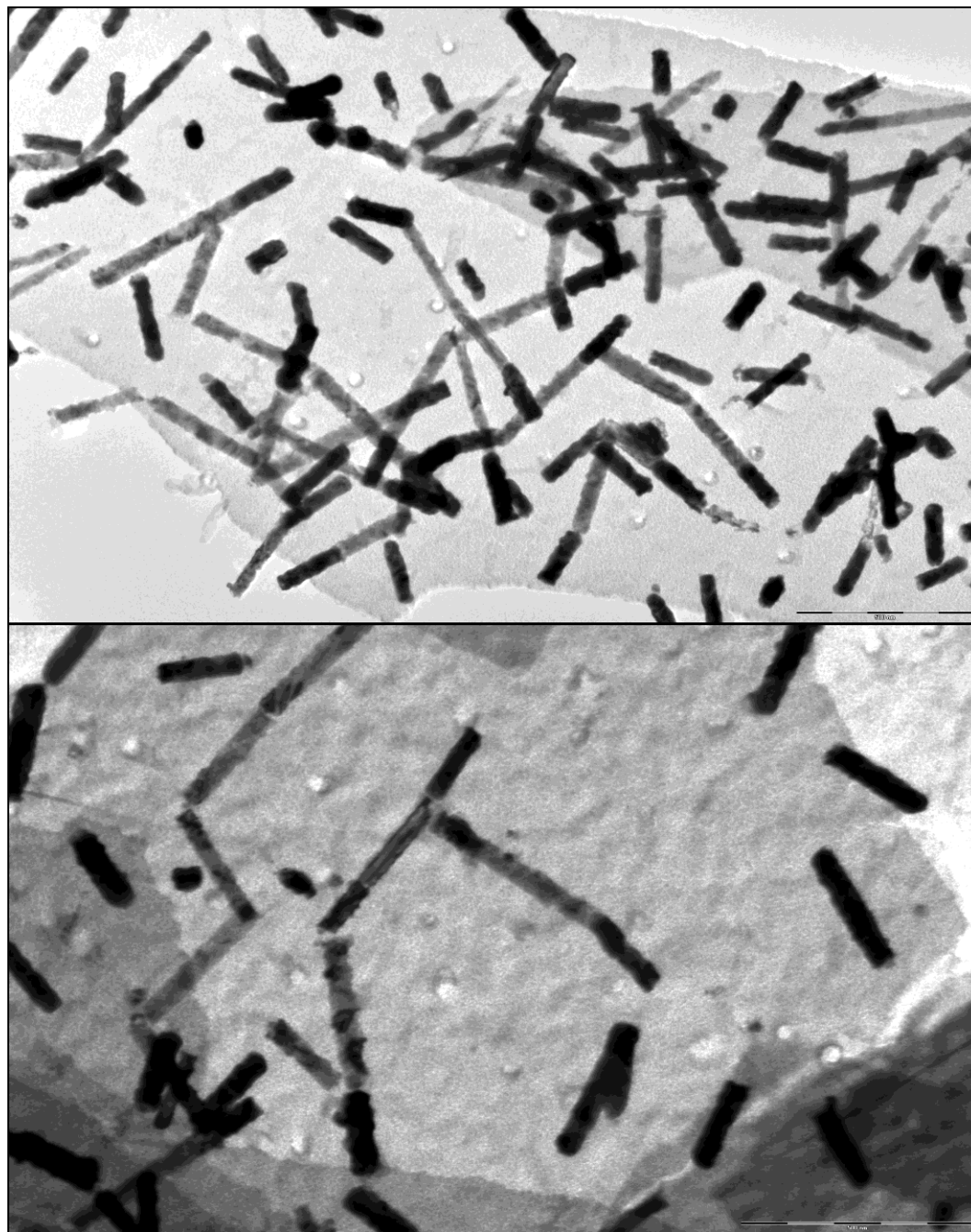


Fig 4.3: TEM image of Ni-Au-Ni-Au segmented nanorods formed under optimized conditions.

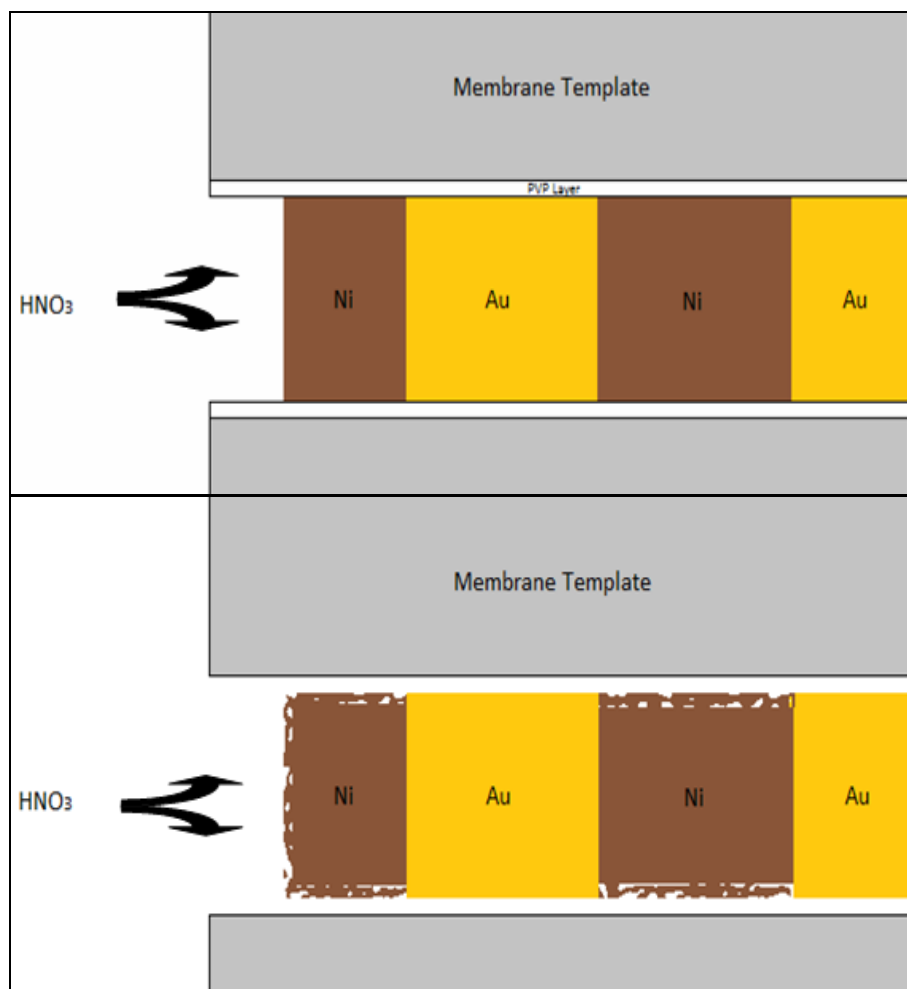


Fig 4.4: Depiction of attack of nickel nanorod segments within the synthesis template by nitric acid (top) before exposure to nitric acid (bottom) after exposure to nitric acid.

In order to test this hypothesis, experiments were performed where segmented nanorods are synthesised under optimised conditions, but without any nitric acid treatment or sonication during or between metal electrodeposition steps. As shown in figure 4.5, nanorods formed under such conditions remain intact, indicating that these two factors are most likely the cause of this problem.

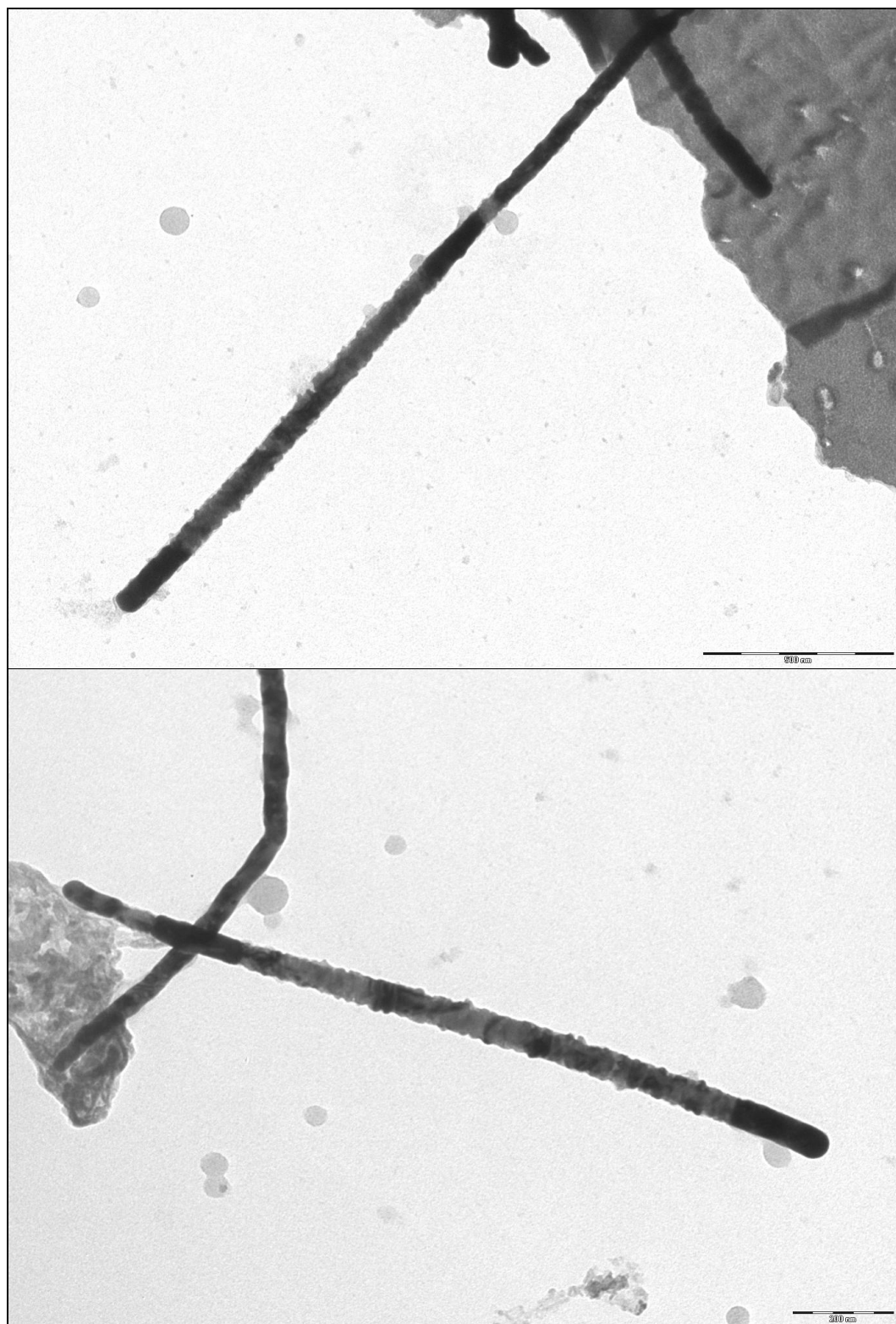


Fig 4.5: TEM image of Ni-Au-Ni-Au segmented nanorods formed under optimized conditions, excluding the use of nitric acid or sonication.

Experiments were then performed to investigate the individual influence of each of these factors upon the synthesis of these segmented nanorods, and to then devise solutions to this problem.

4.3.2.1. Nitric Acid

Segmented nanorods synthesised under optimised conditions, where the nanorods were treated with nitric acid but without sonication, are shown in figure 4.6. In this sample, both intact nanorods and nanorods with missing segments are seen, indicating that the nitric acid treatment contributes to the breakdown of the nanorods as described previously.

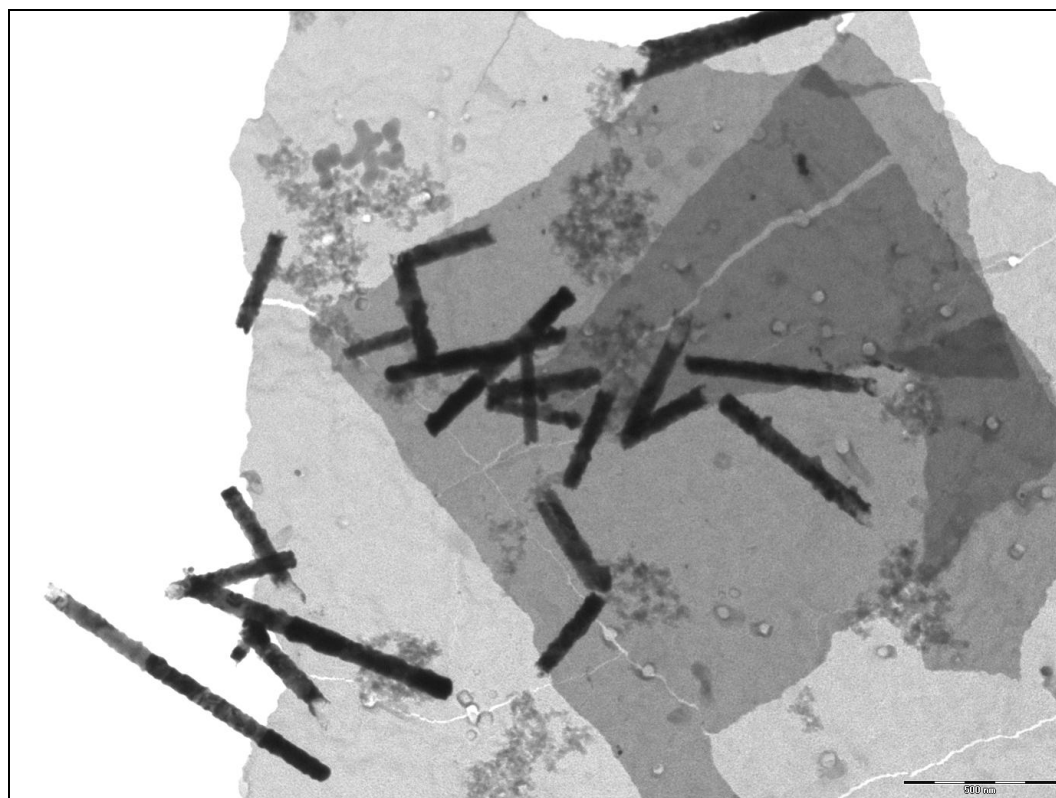


Fig 4.6: TEM image of Ni-Au-Ni-Au segmented nanorods formed under optimized conditions, excluding the use of sonication.

There are a number of ways by which this problem could be circumvented. One method involves the use of a conductive material other than silver, which is then removed with a chemical that does not attack either nickel or gold. However, this forgoes the advantages of using silver as the backing material. An alternative method involves the deposition of a smaller quantity of silver into the membrane prior to depositing the nanorod metal. However, this procedure may prove insufficient to seal all of the membrane pores. A further solution is to employ various methods for removing the silver, in particular, the use of a chemical agent that will dissolve the silver, but not react with the nickel or gold.

One such solution is a mixture comprised of 4 parts methanol, 1 part 30% ammonia solution and 1 part 30% hydrogen peroxide solution. Brief treatment (~2 min) of the synthesis membrane containing the nanorods with such a solution is sufficient to remove all deposited silver (signified by a change in the membrane colour from grey to brown), but is not so long that the membrane is degraded to any significant extent. TEM images of nanorods collected after such treatment (fig 4.7) show that this method yields a vast majority of intact nanorods (comparable to when no nitric acid is used), with no deposited silver present. Thus, this solution will be used instead of nitric acid in a revised, optimised procedure for the synthesis of multi-segmented nanorods.

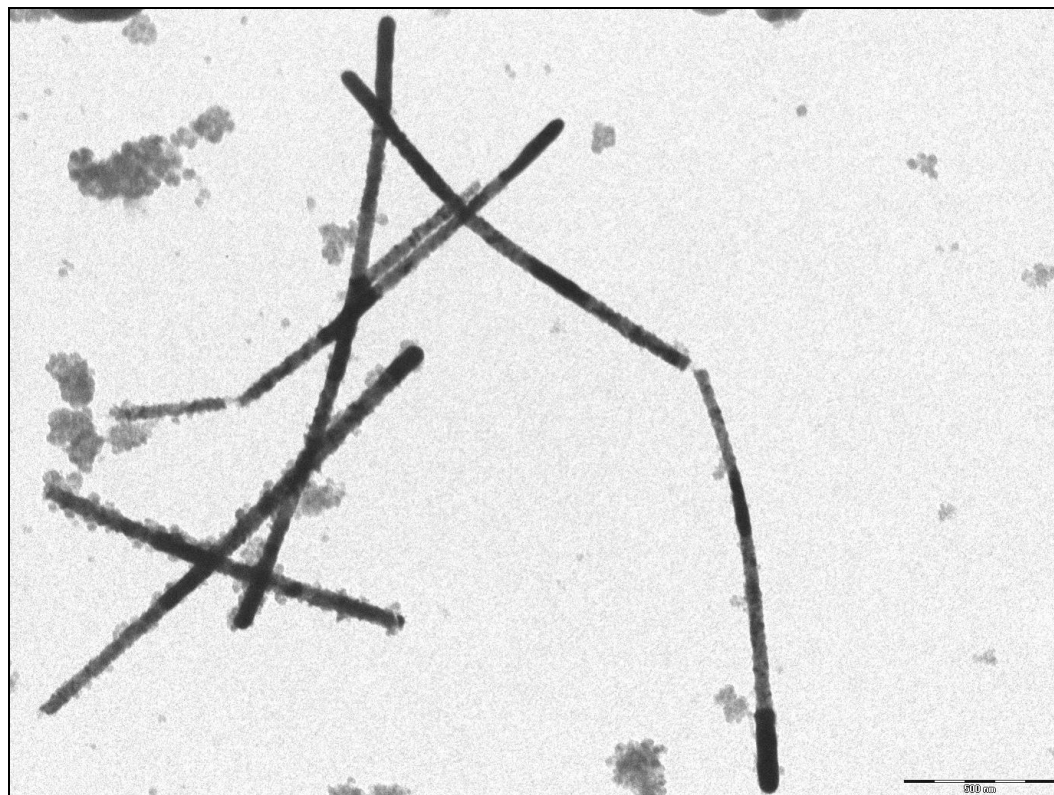


Fig 4.7: TEM image of Ni-Au-Ni-Au segmented nanorods formed under optimized conditions, with no sonication and treatment with 4:1:1 methanol:30% NH_3 :30% H_2O_2 to remove deposited silver.

4.3.2.2. Sonication

Segmented nanorods synthesised under the revised optimised conditions, where sonication is now used and 4:1:1 methanol : 30% NH_3 : 30% H_2O_2 is used in lieu of nitric acid, are shown in figure 4.8. The added use of sonication appears to yield a large number of broken nanorods, much in the same way as when the segmented nanorods were previously treated with nitric acid.

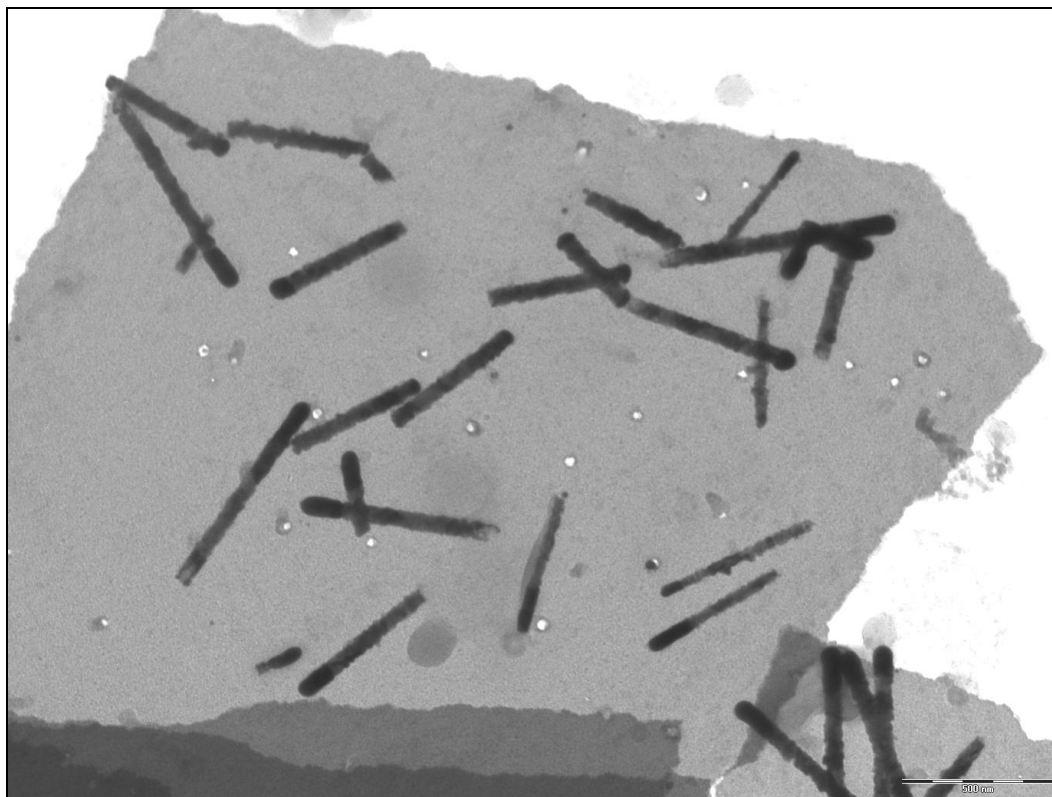


Fig 4.8: TEM image of Ni-Au-Ni-Au segmented nanorods formed under optimized conditions, with sonication and treatment with 4:1:1 methanol:30% NH_3 :30% H_2O_2 to remove deposited silver.

Such sonication also results in a much wider range of nanorod segment sizes, in contrast with the results presented in chapter 3 which indicated that sonication during and between metal deposition steps acts to improve the uniformity of metal deposition. This may be explained by considering that when such nanorods break during sonication i.e. during synthesis, these nanorods are no longer in electrical contact with the silver backing, such that no further metal electrodeposition can occur within these pores. More metal deposition then occurs within the pores which remain electrically connected to the silver backing (for a given passed charge), resulting in a large range of nanorod segment sizes and number of deposited metal segments. This explanation is supported by current vs. time data for the metal depositions, which shows a quicker drop from the initial steady current for subsequent depositions (fig 4.9). Such an effect would occur if the total surface area over which metal is deposited is reduced

(less capacitive charging required and smaller faradaic current due to electrodeposition), as would certainly be the case if a large number of pores are electrically disconnected from the silver backing.

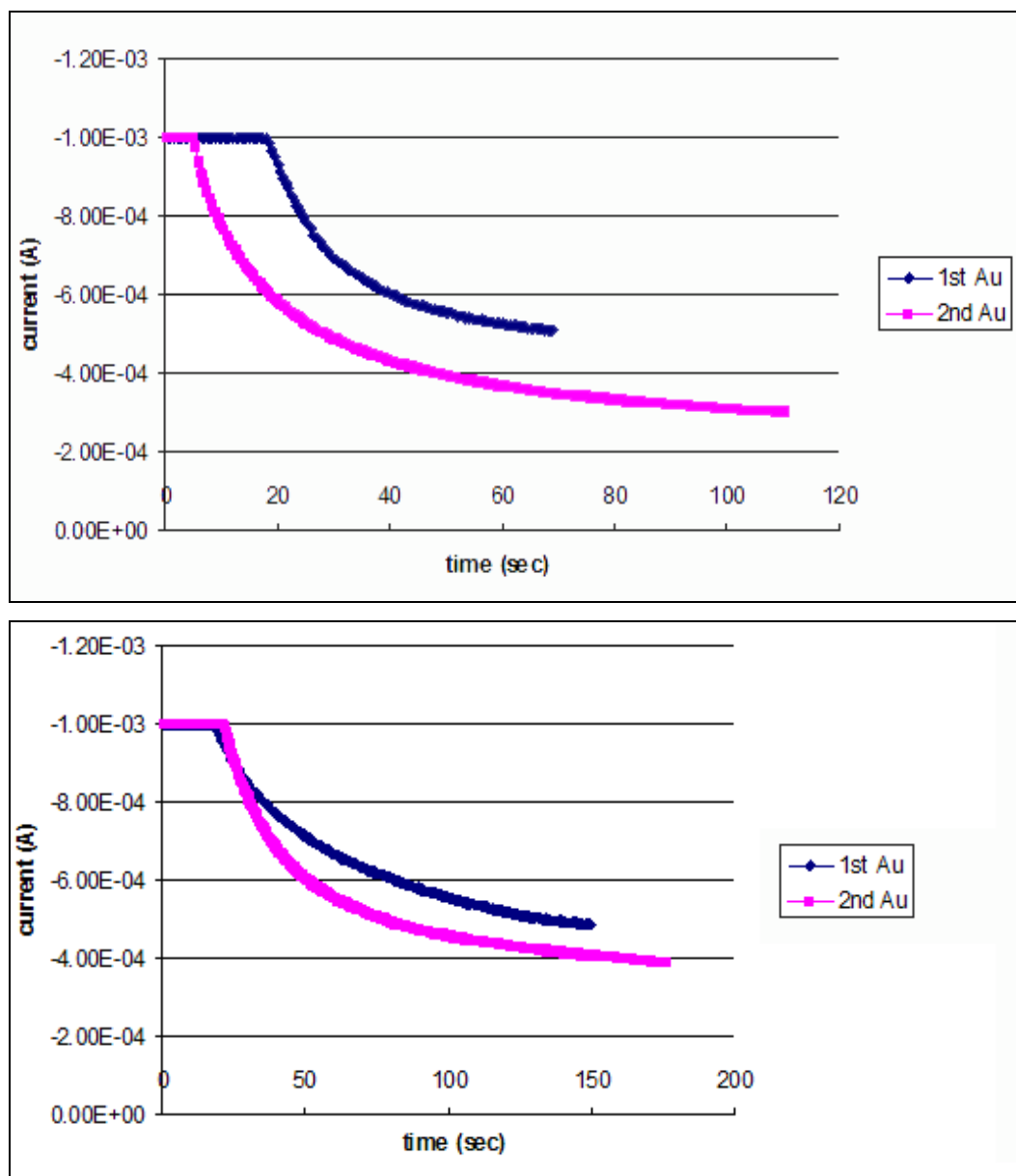


Fig 4.9: current vs. time data for the deposition of subsequent gold segments in a Ni-Au-Ni-Au sample (top) with sonication (bottom) without sonication.

Clearly, the use of sonication, while beneficial for single segment nanorods, is detrimental to the formation of multi-segment nanorods. Thus, sonication was not employed in any further synthesis of multi-segmented nanorods.

4.3.3. Nanorod Length vs. Charge

Using the final revised version of the synthesis procedure, bi-segmented Ni-Au nanorods comprised of segments formed from a variety of passed charges were then formed, in order to determine the relationship between passed charge and segment length under these conditions (fig 4.10 – 4.12).

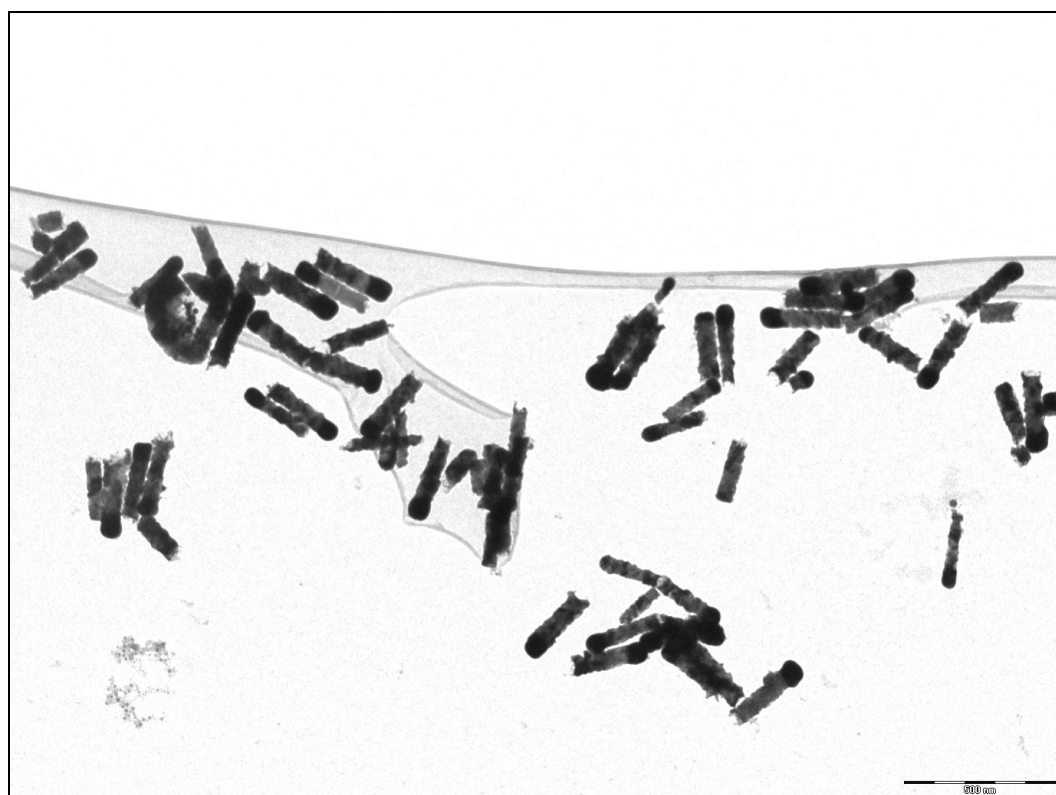


Fig 4.10: TEM image of (0.08C) Ni – (0.08C) Au nanorods.

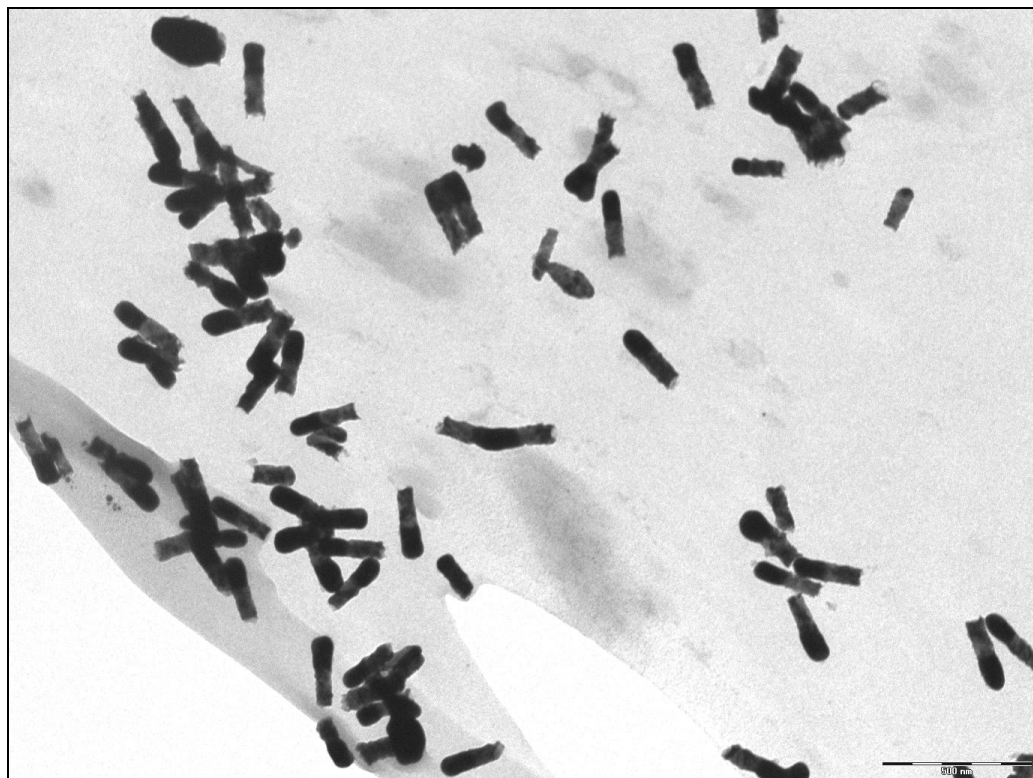


Fig 4.11: TEM image of (0.06C) Ni – (0.12C) Au nanorods.

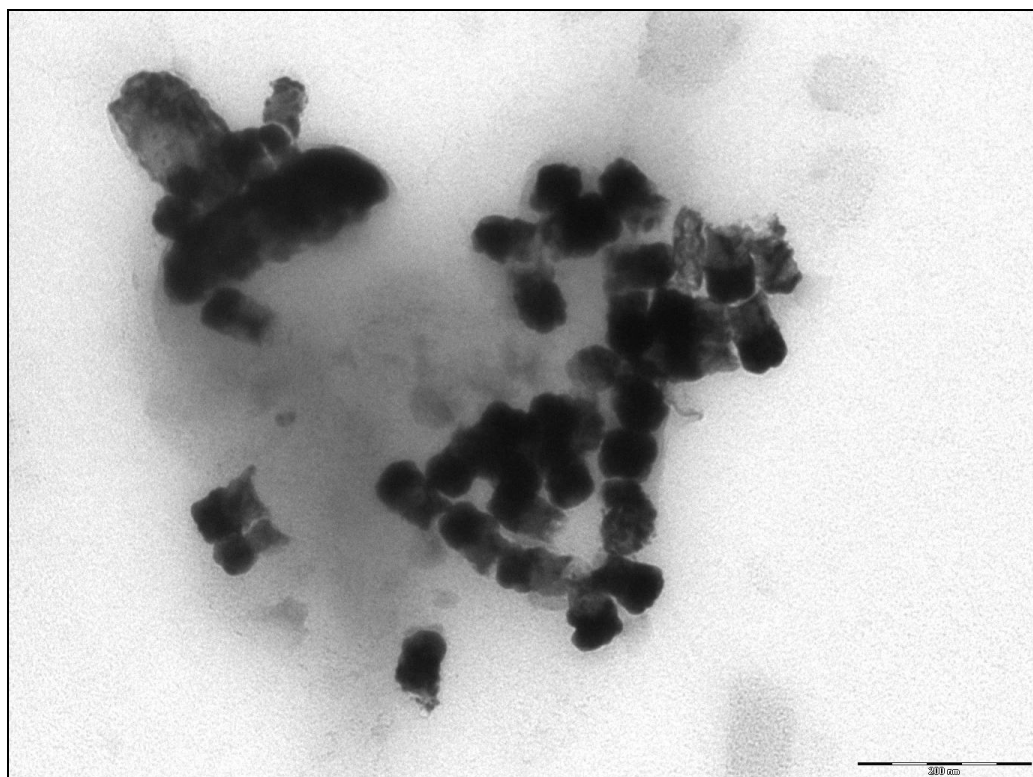


Fig 4.12: TEM image of (0.04C) Ni – (0.04C) Au nanorods.

From such images (fig 4.10 – 4.12), average segment lengths (from at least 100 measurements) were determined, and the results plotted as shown in fig 4.13.

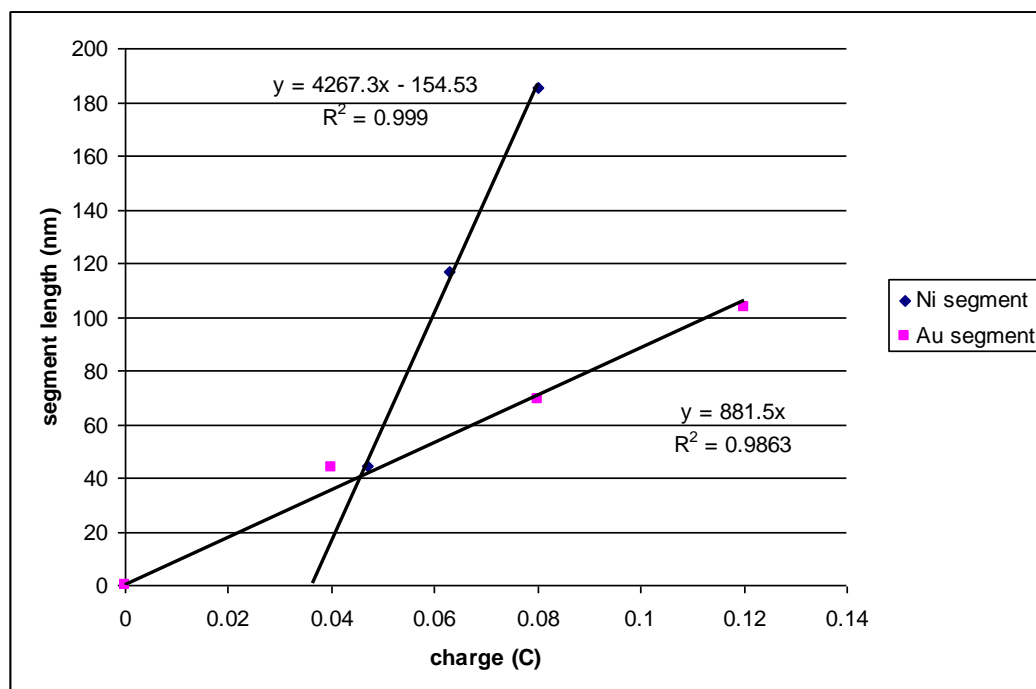


Fig 4.13: TEM image of (0.04C) Ni – (0.04C) Au nanorods.

As expected, there clearly exists a linear relationship between the charge passed and the amount of metal deposited. While for gold this relationship passes through the origin of the graph as one would expect, the nickel deposition does not, passing instead through the charge axis at 0.036C. This result may be explained by considering that residual silver in the pores from the first metal deposition is deposited prior to the nickel (due to the large differences in reduction potential between these two metals). This would effectively result in an “induction” period for the nickel deposition, which will not commence until a sufficient amount of charge has passed to deposit the residual silver species. This induction period does not occur for the concurrent gold deposition onto the nickel segment, as any residual nickel species in the pores are rendered insoluble due to the pH of the gold plating solution.

Although these results were collected for the formation of bi-segmented nanorods, these relationships between passed charge and segment length are anticipated to hold for nanorods made from three or more segments of gold and nickel. A number of key differences will however need to be taken into account. Firstly, subsequent nickel deposition onto gold will be anticipated to have no induction period, as no codeposition with gold takes place. Secondly, the kinetics of electrodeposition may differ for depositions on different metal bases i.e. the deposition of nickel on silver will not necessarily have the same kinetics as the deposition of nickel on gold. However, this difference is anticipated to be minor, as any difference in kinetics will only affect the deposition of the initial thin interfacial metal deposit; subsequent deposition will be of nickel upon nickel (though possibly with a different initial crystal structure). [3-4] Thirdly, it has been observed that the membrane pores appear to widen within the depth of the membrane template, meaning that for a given amount of deposited metal, the segments will be shorter. This may be corrected by extrapolating the volume of metal deposited from the above data, and then taking into account the wider pore diameter at the depth of the pores, where deposition takes place.

4.3.4. Final Synthesis Conditions

In order to confirm that segmented nanorods with properties suitable for use with block copolymer templates may be synthesised using the combination of the revised synthesis procedure for segmented nanorods, together with the polymer removal method developed in chapter 3, nanorods (0.04C – 0.04C Au-Ni) were formed (under conditions listed below) and examined by TEM.

Conditions

- Synthesis template prepared **without** a chromium adhesion layer.

As mentioned in the introduction to chapter 3, this layer is beneficial in studying the nanorods but is undesirable in nanorod samples that are to be eventually included into block copolymer templates as such a layer cannot be dissolved or otherwise removed.

- Nanorods are synthesised using the procedure as optimised for *segmented* nanorods in this chapter:
 - Specific order of metal deposition; silver – nickel – gold – nickel – gold etc.
 - Metal deposition rate controlled by imposing an external current limit. In the case of gold, this limit is 1mA. No current limit is applied in the case of nickel deposition, as limiting the current in this case will result in an undesirable decrease in current density.
 - Removal of the outer edge of the deposition area to account for variations in electric field strength over the cathode.
 - Removal of sacrificial silver through treatment with 4:1:1 methanol:30% NH₃:30% H₂O₂ in lieu of nitric acid.
 - No sonication.

- Removal of polymeric synthesis template by treatment with 3ml of 30% ammonia solution for 1 hour followed by addition of 3ml of 30% hydrogen peroxide solution and standing for 1 hour. Nanorods are then collected by centrifugation.

Results

A stable pellet of nanorods for collection by centrifugation took significantly longer to form (~24 hours) than when residual polymer or the chromium adhesion layer is present (~ ½ hour).

TEM of the resulting nanorod samples show Ni only segments (confirmed by EDAX) of approximately the same dimensions as expected for the amount of passed charge, with no sign of gold segments in the samples (fig 4.14).

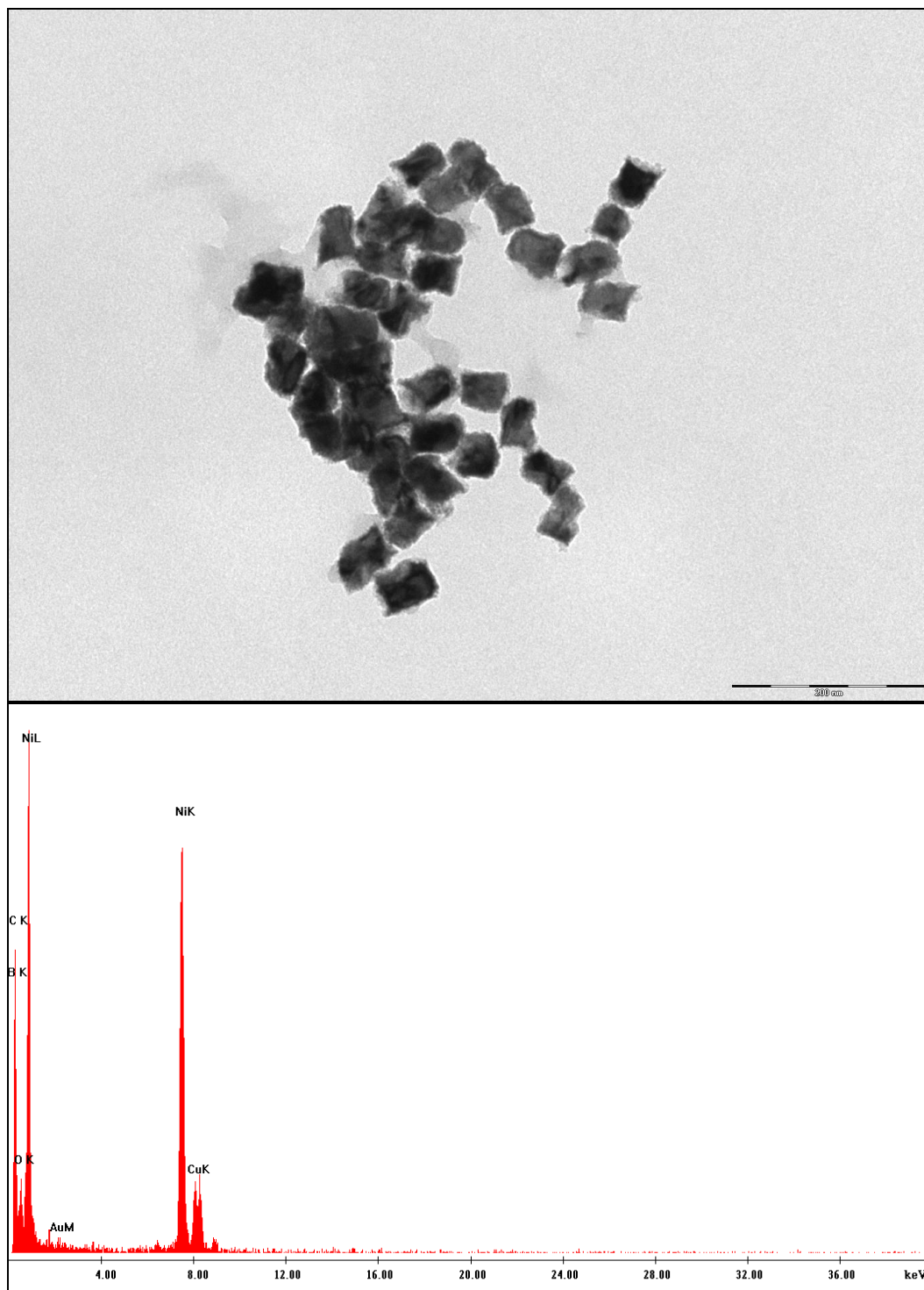


Fig 4.14: (top) TEM image of Au-Ni nanorods treated under conditions optimized for use with block copolymers (bottom) EDAX analysis of the observed nanoparticles.

Small quantities of residual polymer (smeared type) also appears to be scattered sparsely over the TEM grid, some of which contains small ($\sim 2\text{-}3$ nm diameter)

electron dense particles (fig 4.15), the composition of which was not identified by EDAX due to the dominating copper signal from the TEM grid. (fig 4.16).

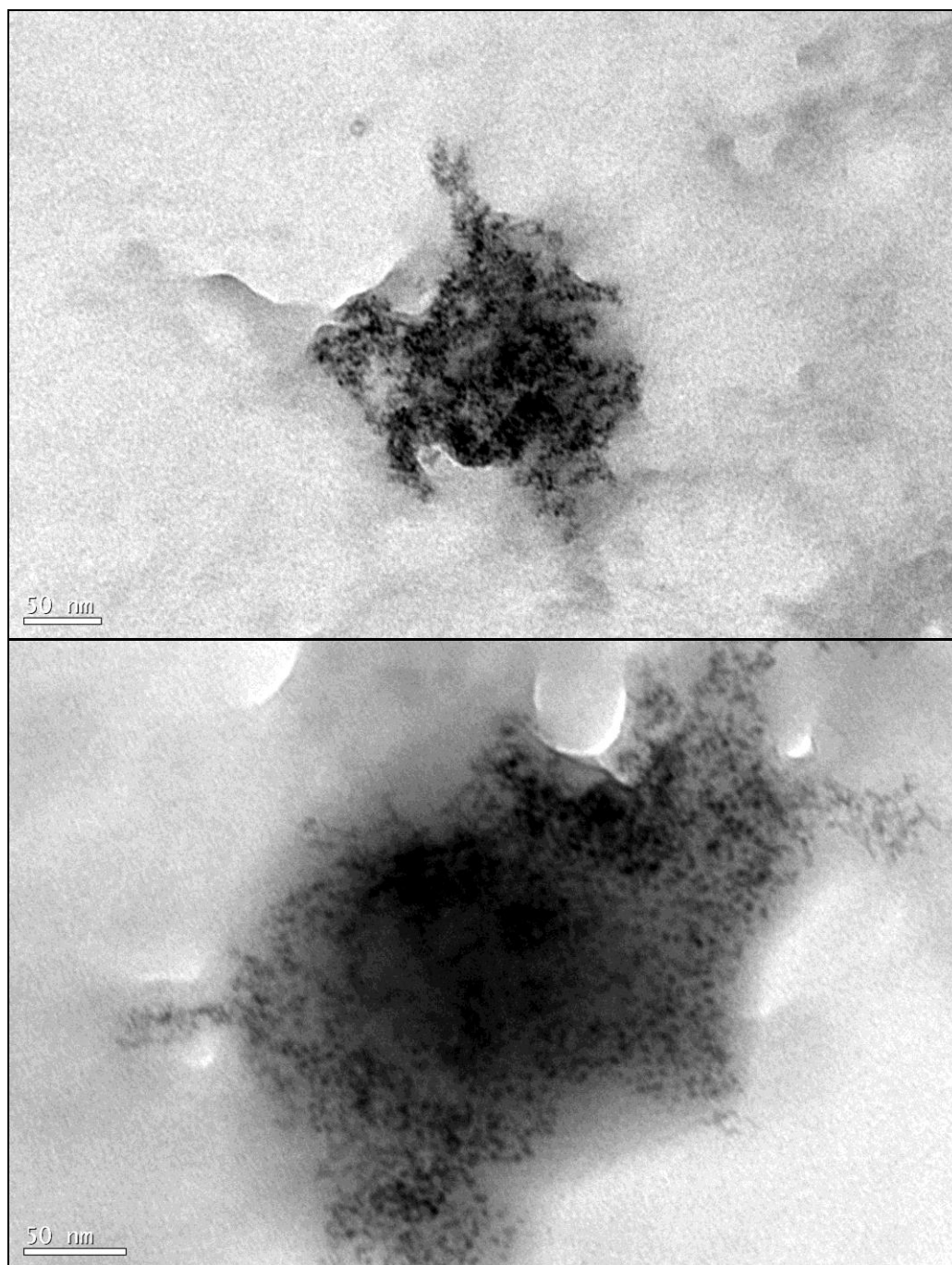


Fig 4.15: TEM images of small particles dispersed within traces of residual polymer.

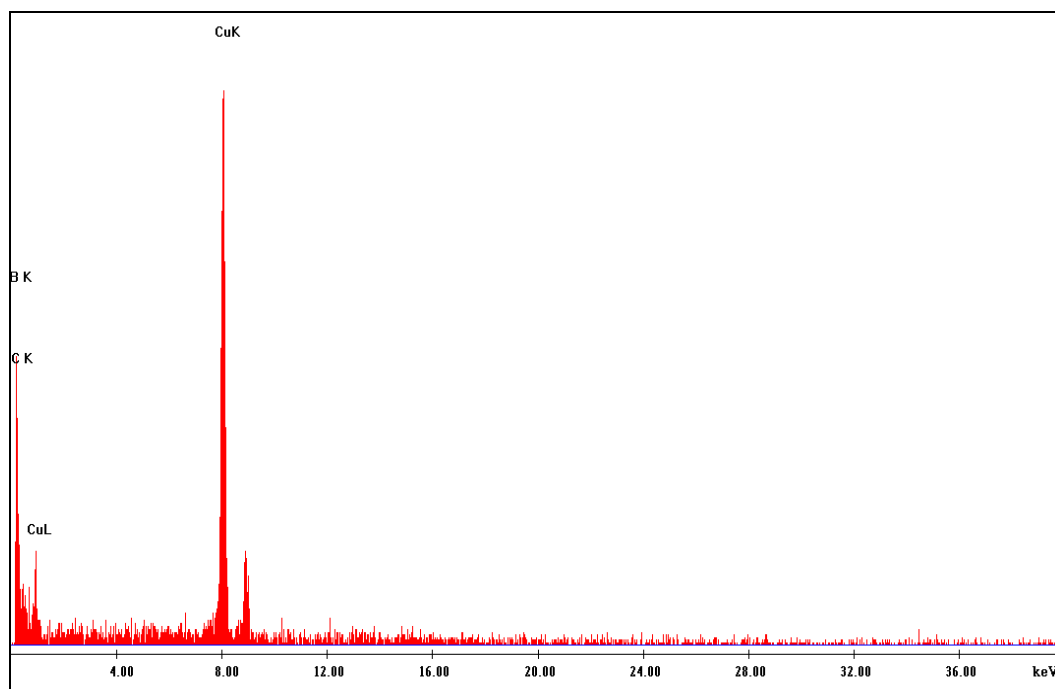


Fig 4.16: EDAX of residue polymer smears containing dispersed particulates as shown in fig 4.15.

Discussion

As the only differences between this procedure and earlier procedures that yield intact nanorods are the lack of a chromium adhesion layer and the use of the ammonia/hydrogen peroxide mixture treatment to remove the polymer template, neither of which is expected to have a *direct* effect upon the nanorods (as the chromium layer is not required during synthesis of the nanorods and the polymer removal treatment is not known to chemically attack either the gold or the nickel segments to any noticeable degree) aside from a longer centrifugation time to sediment them, these observations are highly unusual. Yet, this observation is made with *all* nanorod samples that are treated in this manner.

Given the disappearance of the gold segments, and the appearance of the small, electron dense particulates that appear to be localised within residual polymer (most likely polyvinylpyrrolidone), the most plausible explanation for this observation is that these small particles could be in fact fragments of the gold

segments. Considering that chemical degradation of the gold appears unlikely based on previous experiments, such fragmentation of gold segments may be a result of the forces applied on collecting the nanorods using centrifugation.

Collecting the nanorods by centrifugation subjects them to a centrifugal force directed away from the axis of rotation, the magnitude of which depends upon the mass of the nanorods (m), the distance from the rotational axis (r) and the rate of rotation (N):¹

$$F = m \cdot r \cdot (2\pi N)^2$$

One consequence of the dependence of this force upon the distance from the rotational axis, is that different parts of the nanorods are then subject to different magnitudes of centrifugal force, resulting in a tension stress experienced over the nanorods.

When a metal is subjected to such a tensile stress, the metal's morphology can change over time in response (deformation); the probability and extent of which scales with the degree of stress applied and length of time over which the metal is subjected to this stress. Although in previous experiments the applied stress didn't appear to be sufficient to cause deformation, in this latter experiment, the probability of deformation is expected to be relatively high (and extensive), as it combines the effects of a high degree of tensile stress (owing to the large difference in mass between the ends of the nanorods) with a necessarily large centrifugation time (arising from the absence of chromium and residual polymer which previously acted to aggregate the nanorods).

¹ The net force applied to the nanorods is in reality a balance between the sedimentation force applied by the centrifuge and that of buoyancy (dependant upon the mass of fluid displaced by the particle) and stokes drag (dependant upon the shape and velocity of the particle) which opposes the sedimentation of the nanorods.

The nature of the resulting metal deformation depends upon the initial metal structure. In the case of both the nickel and gold nanorod segments, which possess a polycrystalline structure as indicated by TEM (fig 4.17) (electrodeposited metal (especially hard metal) [5] is typically polycrystalline in nature² [6-7]) there are two possible types of permanent change in morphology that may occur; fracture and plastic deformation. Fracture involves the initiation and propagation of cracks in a material through the breakage of metallic bonds, to the extent that the material breaks apart. Plastic deformation on the other hand involves the propagation of dislocations (defects within the crystal lattice structure) by the rearrangement of metallic bonds, in order to allow the metal to flow in response to the applied stress. The dominant deformation mechanism is determined principally by the hardness of the metal. Hard metals (such as Ni) tend to undergo fracture (brittle) before plastically deforming, whereas soft metals (like Au) tend to plastically deform (ductile) before any fracture can occur. The hardness of a metal is determined by the (a) strength of the metallic bonds (weaker bonds are more easily broken and reformed thereby allowing changes in metallic structure to occur more easily) and (b) the extent to which dislocations can propagate throughout the structure. Decreasing grain size, the presence of impurities in the lattice and a high density of dislocations all typically serve to impede the propagation of dislocations, thereby increasing the hardness of a metal.

Interestingly, despite being a soft metal, gold segments here seem to have undergone brittle fracture rather than plastic deformation. This brittle fracture occurs at stresses lower than required to deform the nickel, implying that the gold segments contain impurities and/or defects in the crystal lattice that both prevent dislocation propagation (and therefore plastic deformation) and decrease fracture toughness (resistance to fracture). Given that the gold bath chemistry is such that the gold should be deposited as soft gold (additives to increase grain size and

² Under specific deposition conditions soft metals such as Au can form mono-crystalline structures when deposited into nanoporous templates. These conditions are not present here. [Wang, J., et al., Journal of Physical Chemistry B, 2004. **108**: p. 841]

reduce defects in addition to the low number of impurities), brittle fracture is only plausible as an explanation if impurities from other sources are co-deposited or occluded within the gold structure. One possible impurity that may yield brittle fracture of the gold segments is insoluble nickel hydroxide (that results from the residual nickel growth species from the previous plating step being exposed to the higher pH of the gold plating solution), which cannot be co-reduced with the gold, but may be occluded within the growing gold structure.

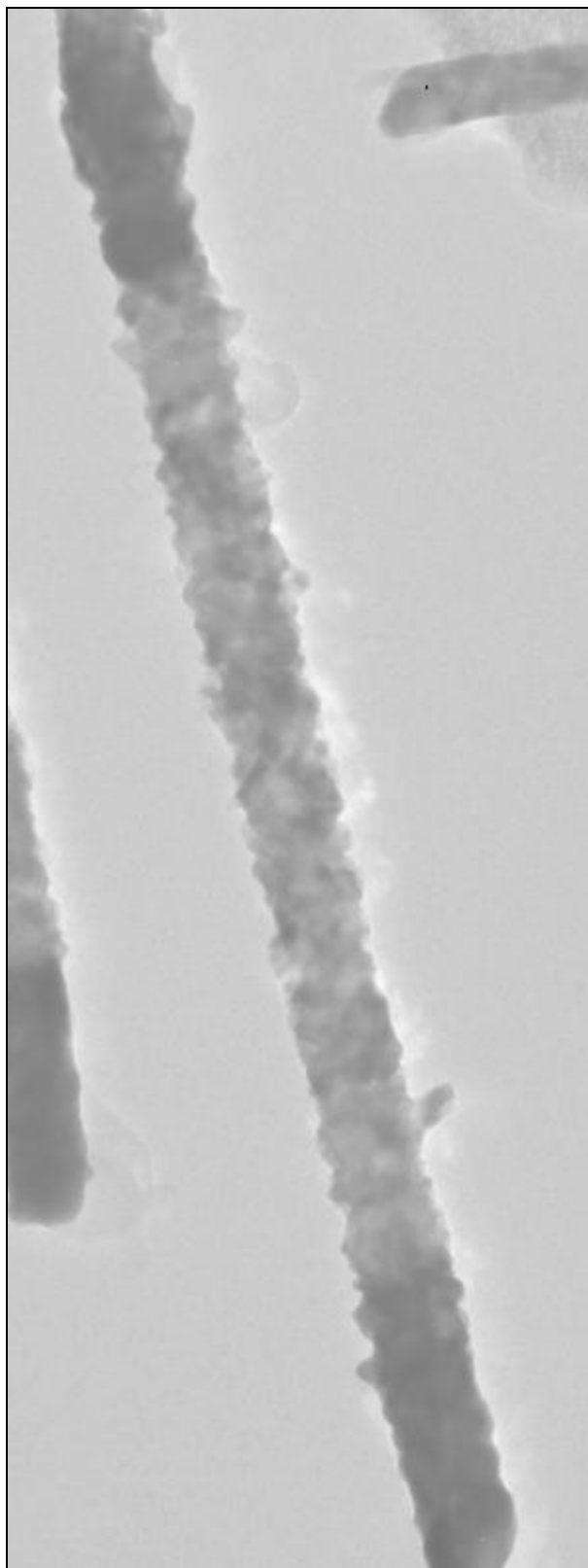


Fig 4.17: TEM of Au-Ni-Au nanorod at 200kV showing the polycrystalline nature of the deposited metal.

One way to test this hypothesis is to examine nanorods subjected to treatment that removes polymer residues, followed by centrifugation for collection *several months* after their synthesis. The idea here is that over this long period of time, redistribution of any possible impurities in the crystal lattice will occur by solid state diffusion, resulting in gold segments that are less susceptible to brittle fracture, and so will behave differently when subjected to centrifugation. Depending upon the nature of the impurities, such diffusion may occur by one of two mechanisms; vacancy diffusion or interstitial diffusion. Interstitial diffusion occurs when the solute atoms are smaller than those comprising the crystalline lattice, and involves the solute atoms moving through the spaces between the crystal lattice atoms. Vacancy diffusion occurs when the solute and lattice atoms are of a similar size and the crystal lattice contains imperfections known as vacancies; missing atoms from the crystal lattice. This form of diffusion involves the migration of the solute atoms by movement of adjacent atoms into those vacancies. This is a relatively slow process compared to interstitial diffusion, although in the case of a polycrystalline solid, vacancy diffusion can occur much quicker via migration along the grain boundaries, which offer much less resistance to diffusion of atoms than diffusion through the crystal lattice or dislocations in the crystal lattice, a result of the smaller number of adjacent atoms and incomplete bonding in these regions. [8] Given that the activation energy for diffusion of impurities through the Ni and Au lattices is likely to be much lower than self diffusion of these metals [9-10], and that in either mechanism, diffusion along the grain boundaries is much easier than into the grains, this results in segregation of these impurities to the grain boundaries. [9] The removal of such impurities from the bulk of the crystal lattice allows dislocations to propagate more easily, thereby leading to plastic deformation rather than brittle fracture. This effect is further magnified by the diffusion of impurities out of the gold grains, which in turn yields a large number of vacancies; a phenomenon known as the Kirkendall effect. Aggregation of these vacancies at the grain boundaries results in the formation of voids in the gold segments, which serve to reduce the

yield strength (a measure of the resistance to deformation) and enhance the extent of plastic deformation. [11]

TEM images of 0.04C-0.04C Au-Ni nanorods synthesised 5 months prior to polymer removal and centrifugation (imaged both before and after this treatment) are shown in fig 4.18 and 4.19. As can be seen, the nanorods remain intact after 5 months at ambient conditions, with no evidence of bulk diffusion between the gold and nickel segments. After treatment however, a majority of the gold segments appear to have undergone plastic deformation rather than brittle fracture. Interestingly, many of the nickel segments also appear to have deformed in this case, becoming narrower and in some cases shorter.

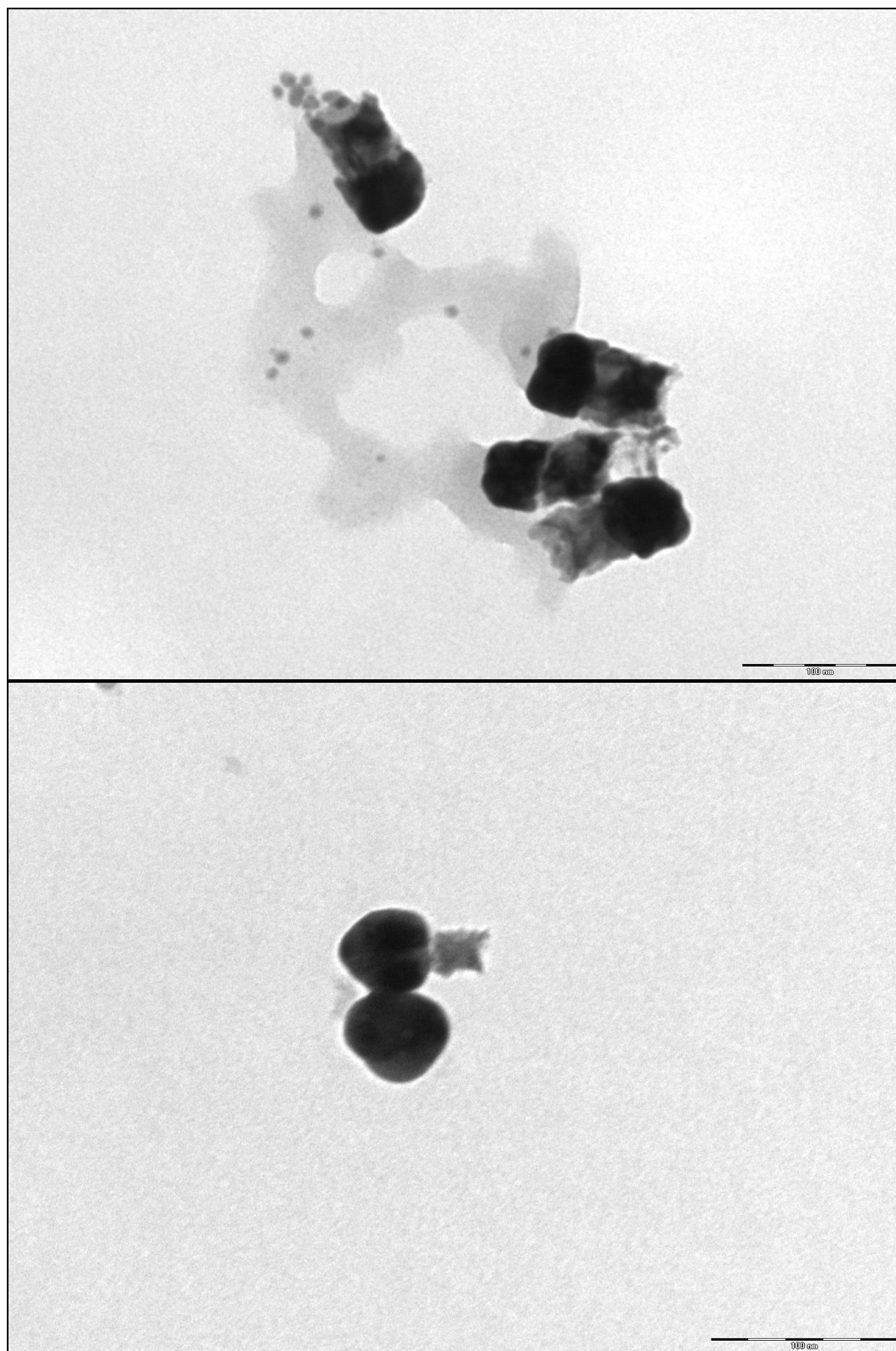


Fig 4.18: TEM of Au-Ni nanorods (top) before polymer removal and centrifugation (bottom) after such treatment.

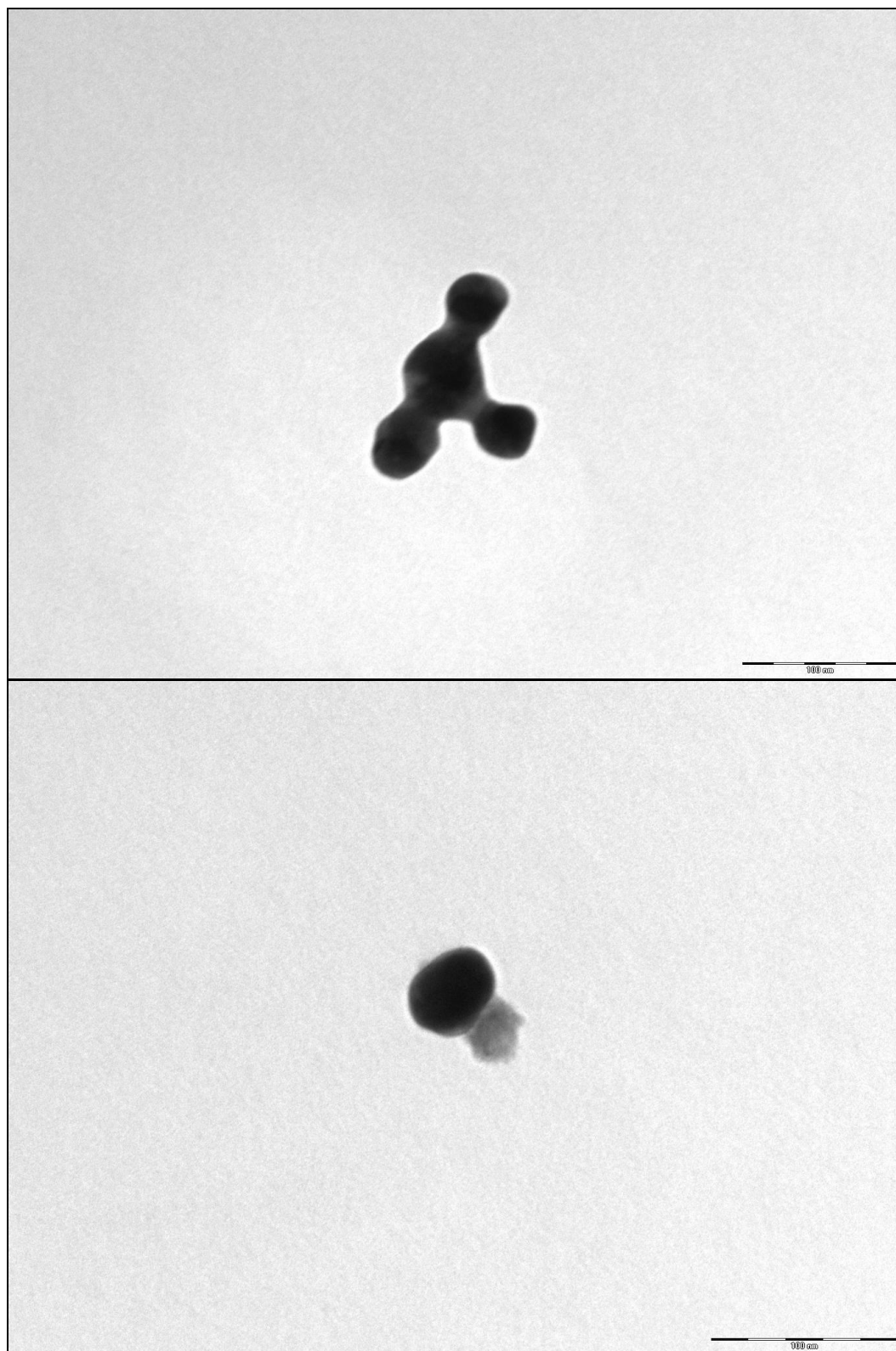


Fig 4.19: TEM of 0.04C-0.04C Au-Ni nanorods after polymer removal and centrifugation.

Examination of long Au-Ni nanorods (100nm long segments) formed and treated under identical conditions also yields evidence of the same deformation mechanisms, with plastically deformed gold segments and thinner nickel segments (fig 4.20 – 4.21). It is observed that adjacent to (or in some cases in place of) the nickel segments are collections of small fragments of low electron density material similar to that of the nickel. Furthermore, intact single segment nanorods of the same dimensions as that of the individual segments are also present (fig 4.22), which is ascribed to breakage of the nanorods at the Au-Ni interface resulting from the greater stresses applied along the nanorods having large nanorod segments.

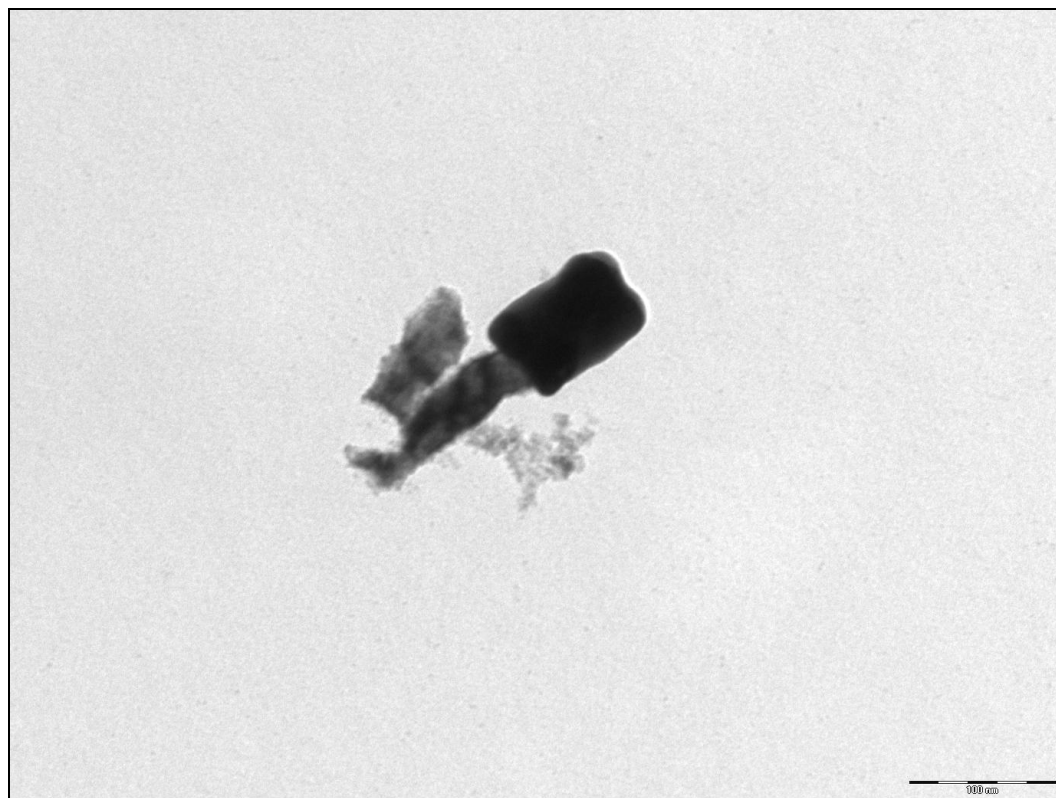


Fig 4.20: TEM of 100nm-100nm long Au-Ni nanorods showing shrinkage of the nickel segment.

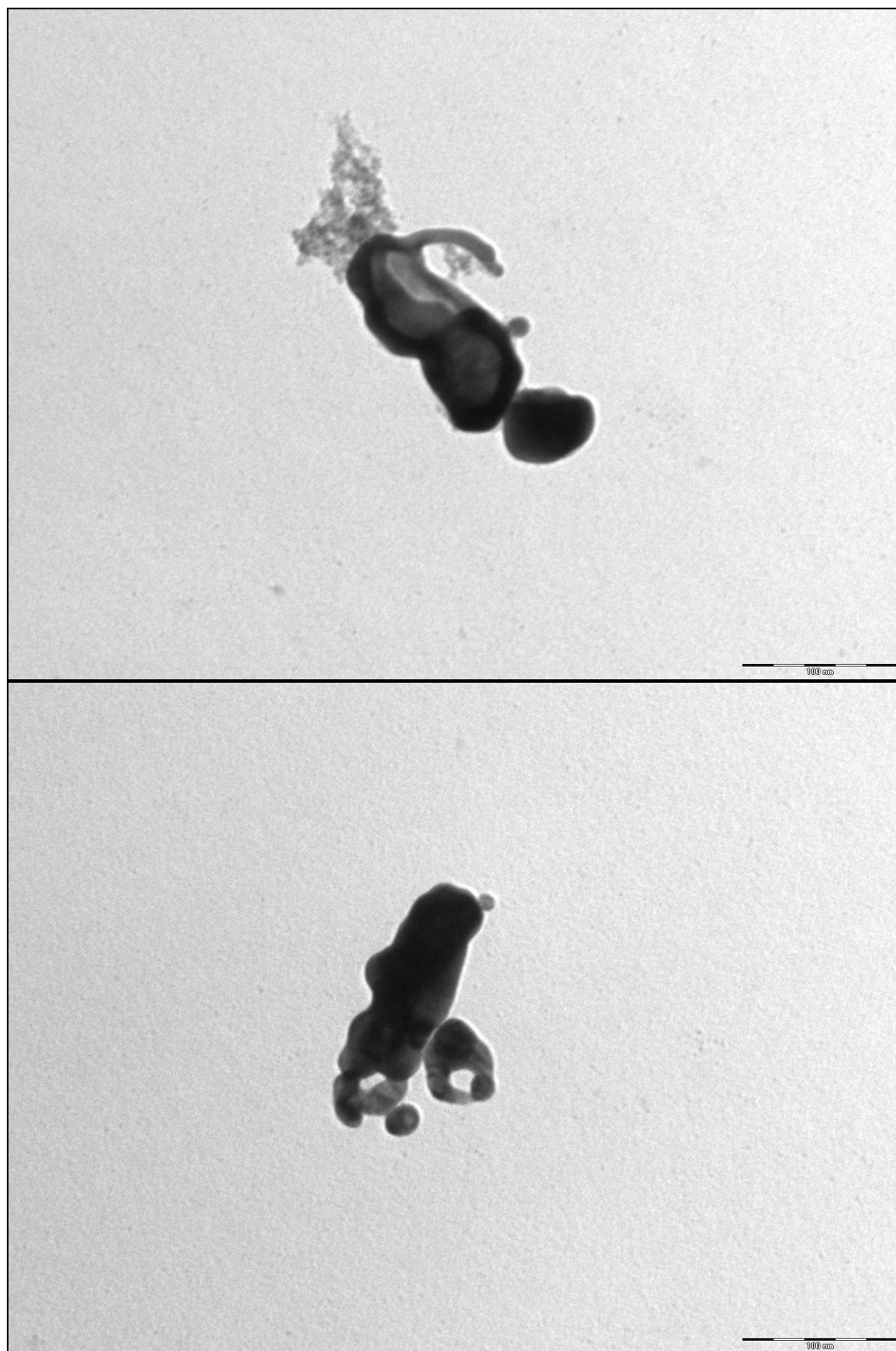


Fig 4.21: TEM of 100nm-100nm long Au-Ni nanorods showing the plastic deformation of the gold segments along with the presence of voids.



Fig 4.22: TEM of 100nm-100nm long Au-Ni nanorods showing the breakage of some of the nanorods into individual segments.

The presence of gold segments undergoing plastic deformation in these aged samples validates the idea that the disappearance of the gold segments in newly synthesised samples results from brittle fracture (through embrittlement from impurities combined with large tensile stresses applied over a sufficiently long centrifugation time). The shrinkage of nickel segments in these aged samples however, is a new effect not observed previously, due to the earlier fragmentation of the gold segments (which in turn reduces the length of time over which the high tensile stress is applied to the nickel segments). The fact that the gold segments remain intact (although deformed) and for the most part attached to the nickel segments in this case, means that the nickel segments are exposed to a higher tensile stress for a longer time, and so leads to much more deformation of the nickel segments.

The deformation of the nickel segments can occur in a number of ways. One such deformation process is diffusional creep, which involves the diffusion of atoms that comprise the crystalline solid such that the grains are able to elongate in the direction of the applied stress, even when the applied stress is smaller than the yield stress of the material. There are two main forms of diffusional creep; Nabarro-Herring creep, which involves diffusion of material through the grains and Coble creep, which involves diffusion of atoms along the grain boundaries. However, this mechanism appears unlikely, as the stress due to centrifugation is not necessarily applied consistently along the length of the nanorod, such that this form of creep would result in a uniform reduction of the Ni segment diameter. Similarly, elongation by grain boundary sliding (where the grains slide past one another in response to an applied stress with some rearrangement of the grain boundaries to accommodate this sliding [12]) is also unlikely, as the applied stress is not necessarily applied along the length of the nanorods. Furthermore, this process is only known to occur at high temperatures, although it may be enabled (or enhanced) by the presence of impurities at the grain boundaries (in particular electronegative impurities) due to a decrease in intergranular cohesion. [13-15] Such impurities may well have diffused into the nickel segment grain boundaries from the gold segment.

An alternative explanation that may account for the observed Ni segment deformation is brittle fracture of the thin (~1nm) amorphous [16] NiO surface layer [17] on the nickel segments, followed by loss of cohesion with the underlying nickel. NiO that forms on the surface of Ni due to oxidation is rather brittle relative to the underlying Ni due to nature of the metal oxide bonding and the presence of large numbers of vacancies [18] and defects [19] in the NiO structure. The tensile force that is applied to the nanorods during centrifugation may be sufficient to induce fracture of this brittle surface layer, with subsequent loss of the material due to lack of cohesion with the underlying Ni. The exposure of the underlying Ni (particularly in the highly oxidising chemical environment present during the treatment procedure) results in oxidation of the exposed Ni to

NiO, thereby allowing this process to be repeated. The presence of impurities (possibly diffused from the gold segment) may serve to enhance these effects, by further embrittling the NiO layer [18] and by reducing the intergranular cohesion between the NiO and Ni as noted before. [13-15] This latter mechanism for the nickel deformation appears to be most plausible, as it would also explain the presence of the granular material adjacent (or possibly attached) to many of the nickel segments.

4.4. Conclusions

In conclusion, it was found that the application of the best synthesis procedure developed in chapter 3 in the synthesis of multi-segment nanorods yields a range of nanorod lengths with varying numbers of gold and nickel segments. This was found to be due to two different effects; (1) weakening of the Au-Ni interface due to slight chemical attack during nitric acid treatment, such that centrifugation breaks the nanorods, and (2) separation of the deposited metal nanorods away from the silver backing during sonication of the electrodeposition cell (while performing electrodeposition and rinsing), thereby severing electrical contact and preventing any further electrodeposition into the membrane pores.

In order to form multi-segmented nanorods with a narrow range of segment lengths, the procedure developed in chapter 3 was further modified to reduce such effects. To avoid the use of nitric acid, an alternative etching solution based on a mixture of ammonia and hydrogen peroxide was used that does not chemically attack the gold or nickel segments. Sonication was also omitted. Nanorods formed using this new procedure were found to have well defined segments and sufficiently narrow ranges of segment length and diameter (at the required segment dimensions) for use with block copolymer templates, while maintaining a high level of control over the segment length.

Finally, to confirm that nanorods suitable for use with the block copolymers can be produced, the combination of the newly revised synthetic procedure together with the improved collection procedure developed in chapter 3 was used.

However, this yielded nanorod samples where the gold segments appeared to have fragmented, leaving the nickel segments intact. This was ascribed to brittle fracture of the gold segments, facilitated by the presence of large numbers of impurities and the forces applied during centrifugation. This hypothesis was validated by the observation of plastic deformation as opposed to the fracture of the gold segments in aged nanorods, where the impurities have had time to diffuse out of the gold grains. This was accompanied by a thinning of the nickel

segments, owing to the longer stressing time afforded by the gold segments remaining intact, and the breakage of a large fraction of the nanorods at the segment interface.

Although the majority of aged multi-segmented nanorods exhibit a high degree of deformation and breakage at the segment interface, some of these nanorods remain intact, with segment dimensions remaining within the range considered suitable for use with the block copolymer templates. Given that the aim of this research is to investigate the possibility of cross-phase alignment of individual segmented nanorods due to their interactions with the block copolymer microphases (rather than the directed *assembly* of an ensemble of identical, monodisperse nanorods into a network structure), these nanorods are still considered to be suitable for use in such studies.

4.5. References

1. Bauer, L.A., Reich, D. H., Meyer, G. J., Langmuir, 2003. **19**: p. 7043.
2. Reiss, B.D., et al., Journal of Electroanalytical Chemistry, 2002. **522**: p. 95.
3. Winand, R., Electrochimica Acta, 1998. **43**: p. 2925.
4. Delplancke, J.L., M. Ongaro, and R. Winand, Journal of Applied Electrochemistry, 1992. **22**: p. 843.
5. Kline, T.R., et al., Inorganic Chemistry, 2006. **45**(19): p. 7555.
6. Whitney, T.M., Jiang, J. S., Searson, P. C., Chien, C. L., Science, 1993. **261**: p. 1316.
7. Xia, Y., Yang, O., Sun, Y., Wu, Y., Mayers, B., Gates, B., Yin, Y., Kim, F., Yan, H., Advanced Materials, 2003. **15**(5): p. 353.
8. Mehrer, H., *Diffusion in Solids: Fundamentals, Methods, Materials, Diffusion-controlled Processes*. 2007: Springer.
9. Yu, H.-C., A. Van der Ven, and K. Thornton, Applied Physics Letters, 2008. **93**: p. 091908.
10. Ning, C. and Y. Zongsen, Journal of Materials Science Letters, 1995. **14**(8): p. 557.
11. Simnad, M.T., Industrial and Engineering Chemistry, 1956. **48**(3): p. 586.
12. Hahn, H., P. Mondal, and K.A. Padmanabhan, Nanostructured Materials, 1997. **9**: p. 603.
13. McMahon Jr, C.J., Interface Science, 2004. **12**: p. 141.
14. Holt, R.T. and W. Wallace, International Metals Reviews, 1976: p. 1.
15. Gibbons, T.B., Materials Science and Technology, 1985. **1**: p. 1033.
16. Marcus, P., *Corrosion Mechanisms in Theory and Practice*. 2 ed. 2002: CRC Press.
17. Payne, B.P., et al., Surfaces and Interfacial Science, 2007. **39**(7): p. 582.
18. Evans, A.G., D. Rajdev, and D.L. Douglass, Oxidation of Metals, 1972. **4**(3): p. 151.

19. MacDougall, B., D.F. Mitchell, and M.J. Graham, *Israel Journal of Chemistry*, 1979. **18**: p. 125.